

Non-cell autonomous influence of MeCP2-deficient glia on neuronal dendritic morphology

Nurit Ballas^{1,2}, Daniel T Lioy^{3,4}, Christopher Grunseich^{1,4} & Gail Mandel^{1,3}

The neurodevelopmental disorder Rett syndrome (RTT) is caused by sporadic mutations in the transcriptional factor methyl-CpG-binding protein 2 (MeCP2). Although it is thought that the primary cause of RTT is cell autonomous, resulting from a lack of functional MeCP2 in neurons, whether non-cell autonomous factors contribute to the disease is unknown. We found that the loss of MeCP2 occurs not only in neurons but also in glial cells of RTT brains. Using an *in vitro* co-culture system, we found that mutant astrocytes from a RTT mouse model, and their conditioned medium, failed to support normal dendritic morphology of either wild-type or mutant hippocampal neurons. Our studies suggest that astrocytes in the RTT brain carrying MeCP2 mutations have a non-cell autonomous effect on neuronal properties, probably as a result of aberrant secretion of soluble factor(s).

RTT is a neurodevelopmental disorder that is caused by sporadic mutations in the X-linked *methyl-CpG-binding protein 2 (MECP2)* gene¹. Girls born with RTT develop normally for 6–18 months, after which they begin to regress, losing speech, motor skills and purposeful hand motions. They also suffer a myriad of other problems, including microcephaly, mental retardation, autism, severe respiratory distress, epileptic seizures and overall retarded growth². MeCP2 mutations in boys usually lead to neonatal encephalopathy and death during the first year of life.

MeCP2 is a member of the methyl-CpG-binding protein family that functions as transcriptional repressors and contains three functional domains: the methyl DNA-binding domain (MBD) that binds to methylated CpG dinucleotides, a transcriptional repressor domain (TRD) that can recruit co-repressors and chromatin remodeling complexes, and the C-terminal domain that facilitates binding to DNA^{3–5}. Repression is mediated, at least in some circumstances, by the recruitment of the co-repressors mSin3A and histone deacetylases (HDACs)^{6,7}. MeCP2 also enhances histone H3 lysine 9 (H3K9) methylation, a modification that is associated with gene silencing⁸. MeCP2 is highly expressed in mature neurons and regulates activity-dependent gene expression^{9,10} by a mechanism that involves calcium-dependent phosphorylation of MeCP2 (ref. 11). Furthermore, MeCP2 is associated with transcriptionally active genomic regions^{12,13} and may also regulate RNA splicing¹⁴, suggesting that complex MeCP2 functions have a role in RTT pathogenesis.

There are several RTT mouse models, each of which contains different mutations in MeCP2 (ref. 15–17). These models recapitulate many characteristic features of RTT, including a normal early developmental period followed by neurological dysfunction and early

mortality. Notably, a conditional knockout that is specific to neural stem/progenitor cells, driven by the *nestin-cre* transgene, results in a phenotype that is similar to the ubiquitous knockout^{15,16}, suggesting that MeCP2 dysfunction in the brain underlies RTT. Furthermore, conditional knockout of MeCP2 in postmitotic neurons driven by the *calcium/calmodulin-dependent protein kinase 2 (Camk2)-cre* transgene results in a similar, although substantially milder, neurological phenotype^{15,18}, indicating that MeCP2 is important in mature neurons. More recent studies have indicated that mice born with RTT can be rescued by reactivation of normal MeCP2 expression^{19,20}, suggesting that the damage that occurs to neurons can be reversed. In addition to the genetic studies, the effects of MeCP2 dysfunction on neuronal structure and function in RTT patients and mice are further supported by several studies showing abnormalities in dendritic arborization^{21,22}, spine density²³, basal synaptic transmission²⁴, excitatory synaptic plasticity^{24–26} and reduced spontaneous cortical activity²⁷.

Although these studies clearly suggest a neuropathology in RTT, whether the pathology is due exclusively to the lack of functional MeCP2 in neurons has not been determined experimentally. We found that MeCP2 is present in the normal brain not only in neurons, but in all types of glia, including astrocytes, oligodendrocyte progenitor cells (OPCs) and oligodendrocytes. Although MeCP2 is clearly expressed in wild-type astrocytes, it is absent in the astrocytes of RTT mouse brains. Using a coculture system based on two genetically distinct mouse models of RTT, we found that MeCP2-null astrocytes are unable to support normal neuronal growth. Furthermore, conditioned media from the *Mecp2*^{−/−} astrocytes phenocopied the astrocytic effect, suggesting that aberrantly secreted factors by the mutant astrocytes cause the neuronal damage. Finally, hippocampal neurons in these cultures

¹Howard Hughes Medical Institute, Department of Neurobiology and Behavior, State University of New York, Stony Brook, New York 11794, USA. ²Department of Biochemistry and Cell Biology, State University of New York, Stony Brook, New York 11794-5215, USA. ³Vollum Institute and Howard Hughes Medical Institute, Oregon Health and Science University, Portland, Oregon 97239, USA. ⁴These authors contributed equally to this work. Correspondence should be addressed to N.B. (nballas@notes.cc.sunysb.edu).

Received 10 November 2008; accepted 13 January 2009; published online 22 February 2009; doi:10.1038/nn.2275

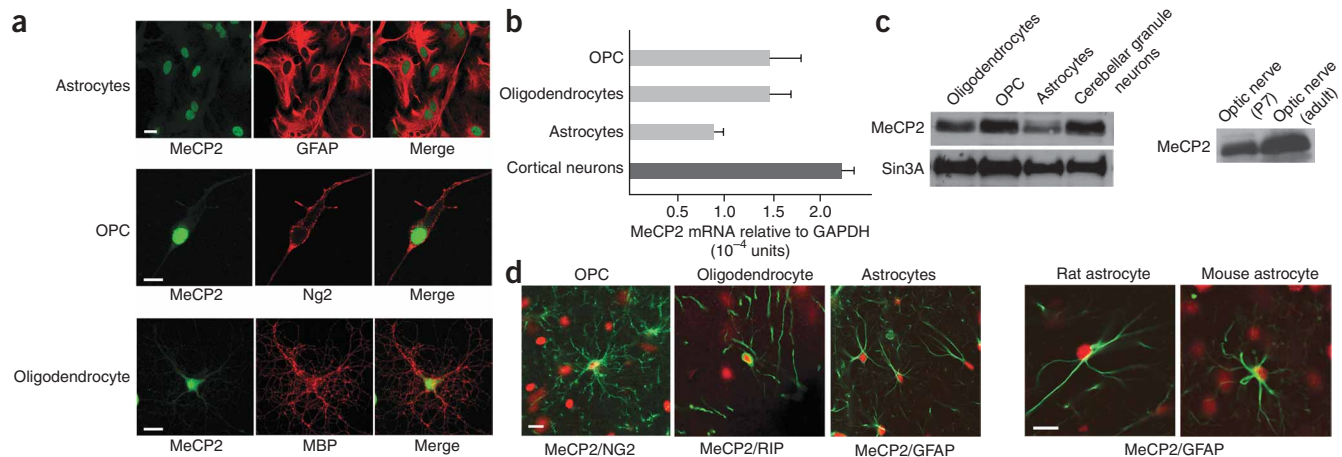


Figure 1 MeCP2 is present in all glial cell types in normal rat and mouse brains. **(a)** Immunostaining indicated that MeCP2 is present in the nuclei of cultured rat glia. MeCP2 protein (green) and cell-specific marker proteins (red) are indicated. Scale bars indicate 20 μ m. **(b)** Real time RT-PCR analysis showing MeCP2 mRNA levels in rat glia. MeCP2 transcripts in cortical neurons are shown for comparison. Error bars represent s.d. on the basis of three independent experiments. **(c)** Western blot analysis showing MeCP2 protein in rat glia (left) and optic nerve (right). MeCP2 and Sin3A migrated at 75 kDa and 150 kDa, respectively. **(d)** Co-immunostaining of rat or mouse brain sections for MeCP2 (red) and the glial-specific markers (green) as indicated. Scale bars indicate 20 μ m.

showed dendritic abnormalities that are observed in RTT patients and RTT mouse models. These findings indicate that MeCP2 dysfunction in glia is probably involved in RTT neuropathology.

RESULTS

MeCP2 is present in the neurons and glia of normal brains

Several previous studies support the notion that, in the nervous system, MeCP2 is present exclusively in neurons on the basis of immunohistochemical analyses indicating that MeCP2 is highly expressed in neurons and undetectable in glia^{17,21,28}. However, because MeCP2 is expressed in many different non-neuronal cell types outside of the nervous system, we sought to examine more systematically whether MeCP2 is expressed in glia, which represent a large non-neuronal cell population in the brain, and provide structural and functional support to neurons. Initially, we asked whether MeCP2 is present in enriched primary cultures of different types of wild-type glia from postnatal brain. Using an antibody directed to the C-terminal peptide of MeCP2, we found that MeCP2 was clearly detected by immunostaining in all glial cell types, including astrocytes, oligodendrocyte progenitor cells and oligodendrocytes (**Fig. 1a**), as determined by staining for the cell-specific markers glial fibrillary acidic protein (GFAP), NG2 proteoglycan and myelin basic protein (MBP), respectively. MeCP2 was also expressed in microglia (data not shown). Quantitative RT-PCR and western blot analyses indicated that, as in neurons, *Mecp2* mRNA and protein were present in all glia (**Fig. 1b,c**) and in astrocytes at somewhat lower levels than other glial types (**Fig. 1a–c**). The relative levels of MeCP2 in glia compared with neurons depend on the type of neurons; although MeCP2 levels in glia and cerebellar granule neurons are comparable (**Fig. 1c**), the levels in cortical or hippocampal neurons are substantially higher (**Supplementary Fig. 1** online). The absence of the neuronal marker Neurofilament-L (**Supplementary Fig. 1**) indicated that the presence of MeCP2 in the different glial cultures is not a result of contamination with neurons in the cultures. MeCP2 in the glial cultures is not an artifact of the enrichment process, as acutely dissociated cerebellar cultures (postnatal day 8, P8; see **Supplementary Methods** online) containing both glia and neurons also showed clear glial-MeCP2 immunostaining (**Supplementary Fig. 2** online).

To determine whether MeCP2 is present in adult glia, we isolated protein from optic nerves, which contain glial, but not neuronal, cell bodies. Western blot analysis revealed that MeCP2 was abundant in early postnatal and adult optic nerve (**Fig. 1c**). Notably, immunostaining of brain sections for MeCP2 and cell-specific markers (**Fig. 1d** and data not shown) indicated that, in addition to optic nerve, MeCP2 was detected in the nuclei of astrocytes, OPCs and oligodendrocytes of adult rat and mouse cerebral cortex. Together, our data clearly indicate that MeCP2 is present not only in neurons, but also in all types of glia in the postnatal brain.

The discrepancy between previous published studies^{17,21,28} and our studies is probably a result of the presence of high levels of MeCP2 in cortical neurons and the relatively low levels in glia, and the efficiency of the antibodies to MeCP2 that were used. When using a commercially available antibody, MeCP2 can indeed be detected in cortical neurons, but not in glia (**Supplementary Fig. 3** online). However, using a more efficient antibody and/or biotin/streptavidin enhancement, MeCP2 can be detected in both neuronal and astrocytic nuclei, although MeCP2 levels in the cortical neurons are higher than in astrocytes (**Supplementary Fig. 3**).

RTT astrocytes cannot support normal neuronal growth

Because MeCP2 is present in the glia of normal brains, we reasoned that the lack of functional MeCP2 in the glia of RTT brains might influence neuronal properties in a non-cell autonomous fashion. We focused on astrocytes, the most abundant non-neuronal cells in the CNS, which are important in neurodegenerative processes²⁹. We first examined whether MeCP2 was absent in the astrocytes of RTT mouse brains. Co-immunostaining for MeCP2 and GFAP on brain sections showed that although MeCP2 is present in the astrocytes of normal brains, it was clearly absent in the astrocytes of RTT brains (**Fig. 2a**). Furthermore, western blot analysis of protein extracts from primary cultures of astrocytes isolated from postnatal brains showed high levels of MeCP2 in wild-type astrocytes and a lack of MeCP2 in RTT astrocytes (**Fig. 2b** and **Supplementary Fig. 1**). The presence of MeCP2 in protein extracts of the wild-type astrocyte cultures is not a result of the presence of neuronal cells in the

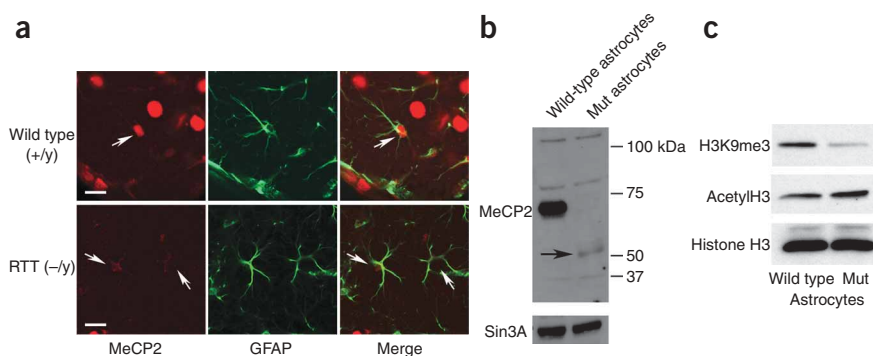


Figure 2 MeCP2 is detected in astrocytes in brain sections from *MeCP2*^{+/-}, but not *MeCP2*^{-/-} mice. (a) Co-immunostaining of brain sections from 6-week-old wild-type (+/y) and RTT (-/y) mice for MeCP2 (red) and GFAP (green). Arrows indicate the presence and absence of MeCP2 in astrocyte nuclei of wild-type and RTT brains, respectively. Scale bars indicate 40 μ m. (b) Western blot analysis confirmed the presence of MeCP2 in wild type and its absence in *MeCP2*^{-/-} astrocytes. Arrow indicates MeCP2 C-terminal peptide product of the recombination event in a previously described mouse model¹⁵. Sin3A served as a loading control. (c) Western blot showing an altered global chromatin signature in astrocytes from RTT mice (Mut). Histones were probed with the indicated antibodies to histone modifications.

cultures, as evidenced by the absence of the neuronal marker Neurofilament-L (Supplementary Fig. 1).

Because MeCP2 recruits the histone-modifying enzymes HDAC and H3K9 methyltransferase, which are often associated with gene repression or silencing, we asked whether MeCP2-deficient astrocytic chromatin was in a derepressed state. We extracted histones from the astrocytes of RTT and wild-type brains and analyzed them by western blot for the presence of acetylated histone H3 and trimethylated lysine 9 on histone H3 (H3K9me3). H3K9me3 was clearly reduced in MeCP2-null astrocytes of RTT male brains compared to astrocytes of wild-type male brains, whereas acetylated histone H3 was elevated (Fig. 2c), consistent with reductions in H3K9 methyltransferase activity or a loss of HDAC activities. Such elevated levels of acetylated histone H3 and reduced levels of tri-methylated lysine 9 on histone H3 were also found in whole RTT brains^{17,30}. These data point to the importance of the presence of MeCP2 in astrocytes for maintaining proper histone modifications and suggest that the changes in histone modifications in MeCP2-null astrocytes to a more permissive state may affect normal astrocytic functions.

To examine whether MeCP2 dysfunction in astrocytes could influence neuronal properties, we exploited a coculture system in which neurons cultured in serum-free medium are exclusively dependent on the presence of an astrocytic feeder layer at short distances from the neurons for their growth^{31,32}. Consistent with previous studies, hippocampal neurons from wild-type mice died after 2–3 d in the absence of astrocytes (data not shown); in the presence of wild-type astrocytes, the neurons appeared to be healthy and extended long and extensive dendritic arbors, as indicated by microtubule-associated protein 2 (MAP2) immunostaining (Fig. 3a,b). However, wild-type hippocampal neurons cocultured with astrocytes from RTT mice were clearly compromised. Specifically, these neurons lacked fine processes and had fewer long processes

(Fig. 3a,b). In addition, MAP2 showed abnormal somal concentrations in many neurons (Fig. 3b), probably as a result of the fewer and shorter dendrites. Only 5% of wild-type neurons showed processes shorter than 50 μ m in length, but up to 40% of the neurons had stunted dendrites of this length when cocultured with astrocytes from RTT mice (Fig. 3c). Although neuronal densities after 3 d in culture were similar (data not shown), after 6 d in the presence of astrocytes from RTT mice, densities were lower by 35% than in the presence of wild-type astrocytes (Supplementary Fig. 4 online). These results suggest that, unlike wild-type astrocytes, MeCP2-null astrocytes cannot support normal neuronal growth, indicating that functional MeCP2 is important in astrocytes for supporting the neurons in the brain.

Using the Golgi staining method to detect dendritic arbors in brain sections from symptomatic RTT and wild-type littermates, we found aberrant neuronal morphologies in the RTT brains that resembled those seen in culture (Supplementary Fig. 5 online). Specifically, CA3 pyramidal neurons in the hippocampus of RTT mice had fewer dendritic branches relative to wild-type CA3 pyramidal neurons (Supplementary Fig. 5). Similar aberrant dendritic morphologies were observed in dentate granule neurons of RTT mice (Supplementary Fig. 5). These data suggest that the abnormal neuronal morphologies in RTT brains are the result of MeCP2 dysfunction and that the aberrant morphologies seen in cultures are not an *in vitro* artifact.

RTT ACM cannot support normal neuronal growth

To examine whether the defects that occur in neurons in the coculture system result from aberrant secretion of soluble factors by the mutant astrocytes, we generated astrocytic conditioned media (ACM).

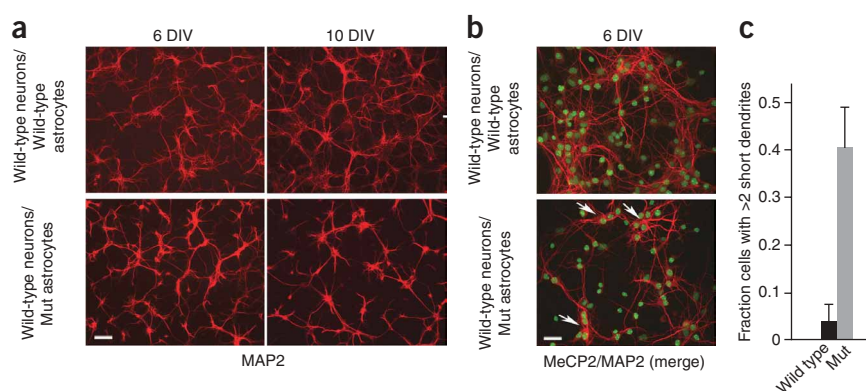


Figure 3 Wild-type hippocampal neurons cocultured with cortical astrocytes from RTT mice have stunted dendrites. (a) Aberrant morphology of hippocampal neurons, visualized by MAP staining (red), increased with time in culture. Wild-type hippocampal neurons cocultured with either wild-type astrocytes (top) or mutant (Mut) astrocytes (bottom). Note the decrease in fine processes and their shorter length of processes when cocultured with mutant astrocytes. Scale bar indicates 100 μ m. (b) Immunostaining for nuclear MeCP2 (green) and MAP2 (red) revealed an aberrant cytoplasmic MAP distribution (arrows) in wild-type hippocampal neurons cocultured with mutant astrocytes. Scale bar indicates 40 μ m. (c) Bar graphs represent the fraction of neurons with at least two short (<50 μ m) dendrites when cocultured with wild-type or mutant astrocytes. Error bars represent s.d. on the basis of three independent experiments.

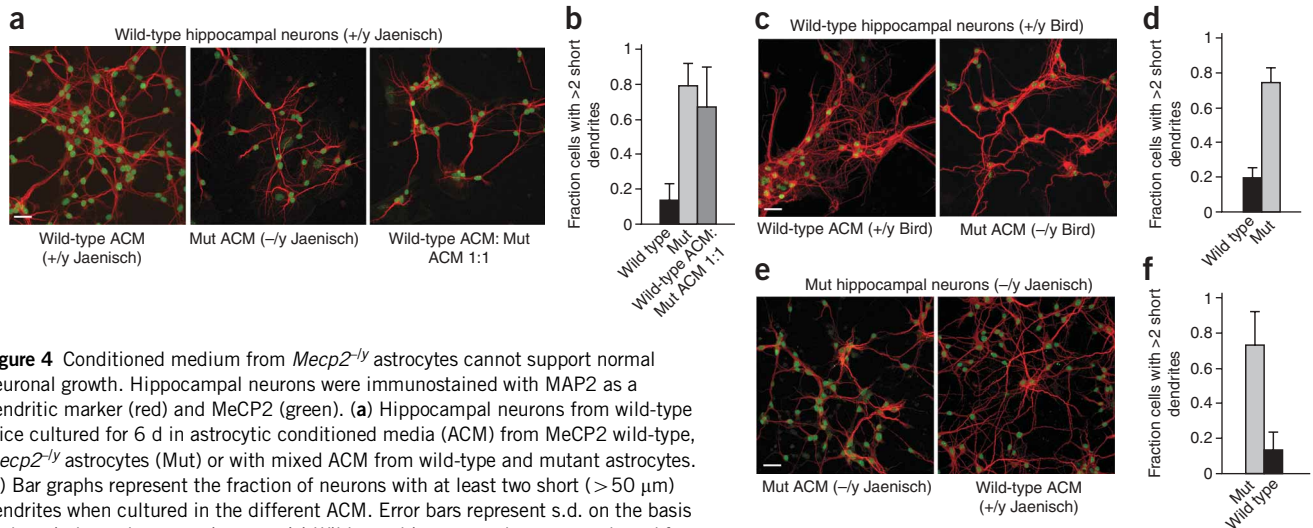


Figure 4 Conditioned medium from *Mecp2*^{-/-} astrocytes cannot support normal neuronal growth. Hippocampal neurons were immunostained with MAP2 as a dendritic marker (red) and MeCP2 (green). **(a)** Hippocampal neurons from wild-type mice cultured for 6 d in astrocytic conditioned media (ACM) from MeCP2 wild-type, *Mecp2*^{-/-} astrocytes (Mut) or with mixed ACM from wild-type and mutant astrocytes. **(b)** Bar graphs represent the fraction of neurons with at least two short (> 50 μ m) dendrites when cultured in the different ACM. Error bars represent s.d. on the basis of three independent experiments. **(c)** Wild-type hippocampal neurons cultured for 7 d with conditioned medium generated from *Mecp2*^{-/-} astrocytes of a previously described mouse model¹⁶ showed similar abnormal morphology. **(d)** Bar graphs as in **b**. **(e)** Hippocampal neurons from RTT mice (Mut) cultured for 6 d were supported by conditioned medium from wild-type astrocytes. **(f)** Bar graphs as in **b**. Note that the gain of image in mutant hippocampal neurons was increased for MeCP2 because *Mecp2*^{-/-} neurons from a previously described mouse model¹⁵ express low levels of the C terminus, which is recognized by the antibody to MeCP2 that we used. Scale bars indicate 40 μ m.

Wild-type hippocampal neurons were cultured with ACM generated from either wild-type or MeCP2-deficient astrocytes and their ability to support neuronal growth was analyzed over a 6-d period (**Fig. 4**). No differences were observed in neuronal growth and morphology over a period of 3 d in culture with or without ACM (data not shown); at later time points, however, conditioned medium from MeCP2-null astrocytes elicited a robust phenotype consisting of stunted dendritic morphology (**Fig. 4a**) and neuronal densities were reduced by 35% (**Supplementary Fig. 4**). We counted the fraction of neurons with short dendrites and found that up to 80% of the neurons cultured in ACM generated by MeCP2-null neurons showed abnormal dendritic morphology, as opposed to only 10–15% of wild-type ACM-treated neurons showing such aberrant morphology (**Fig. 4b**). Mixing the wild-type and mutant ACM in a 1:1 ratio resulted in similar dendritic defects (**Fig. 4a,b**), suggesting that the heterozygous mutations in MeCP2 that occur in RTT patients and which also result in mosaic expression of MeCP2 in glia probably affect the neurons similarly.

To verify that the effects of *Mecp2* mutant astrocytes on neurons are not specific to one type of MeCP2 mutation, but instead represent a general characteristic of dysfunctional MeCP2 in astrocytes, we analyzed a mouse model that carries a different mutation in MeCP2 (ref. 16). We first examined the wild-type and RTT astrocytes of this mouse model for the presence and absence of MeCP2, respectively. Immunohistochemistry of brain sections of 6-week-old littermates showed that MeCP2 is absent in the astrocytes of RTT brains, although it is clearly present in the nuclei of astrocytes of wild-type brains (**Supplementary Fig. 6** online). Furthermore, western blot analysis revealed that MeCP2 is absent in protein extract from mutant

astrocytes, but is clearly present in wild-type astrocytes (**Supplementary Fig. 6**). We generated conditioned media from primary cultures of astrocytes of this mouse model and analyzed their ability to support neuronal growth. Similar to the results with the first mouse model, conditioned medium generated from MeCP2-null astrocytes was unable to support normal neuronal growth (**Fig. 4c,d**). Over 70% of the neurons had short dendrites, as compared with 20% of the neurons when they were cultured in wild-type ACM (**Fig. 4d**). In this case, however, although we noticed some cell death, it was statistically insignificant ($P = 0.26$; **Supplementary Fig. 4**), indicating that the

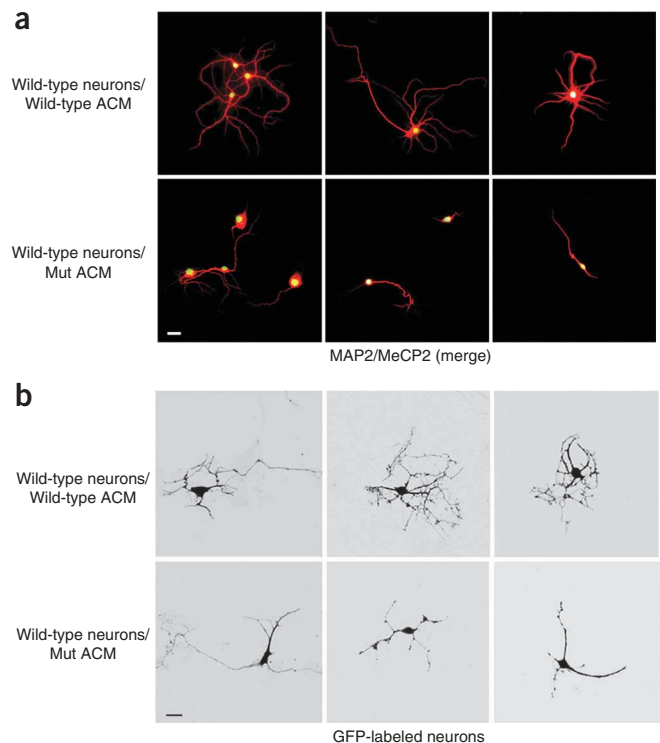


Figure 5 Altered morphology of wild-type neurons cultured with ACM from *Mecp2*^{-/-} astrocytes is evident at the single cell level. **(a)** Immunostaining in low-density neuronal cultures (6 DIV) with MAP2 (red) and MeCP2 (green) revealed aberrant process morphology when the neurons were cultured in ACM from mutant astrocytes (compare top panels, wild-type ACM, with lower panels, Mut ACM). Scale bars indicate 30 μ m. **(b)** GFP-expressing neurons showed aberrant processes when cultured in mutant ACM (compare top panels, wild-type ACM, with lower panels, Mut ACM). Scale bars indicate 20 μ m.

aberrant neuronal morphology conferred by the mutant astrocytes is independent of cell densities or survival.

To further eliminate the possibility that neuronal density may underlie the aberrant neuronal morphology by MeCP2-null astrocytes or their conditioned medium, we prepared low-density cultures of hippocampal neurons. Where individual neurons could be visualized, aberrant dendritic morphology was evident when cultured with conditioned medium from mutant astrocytes, but not wild-type astrocytes (Fig. 5a). Thus, the inability of MeCP2-null astrocytes to support normal neuronal morphology is independent of neuronal cell densities. In addition, to visualize dendritic morphology of single neurons cultured at normal density, we transfected hippocampal neurons with a GFP-expressing vector and examined the cultures 6 d after transfection (Fig. 5b). We found that 70% of the GFP-expressing neurons had stunted processes when cultured with conditioned medium from mutant astrocytes, whereas only 15% showed similar morphology with wild-type conditioned medium. Therefore, the changes that we detected in neuronal morphology using MAP2 staining are reflected at the single cell level.

Finally, we asked whether MeCP2-null neurons are supported by conditioned medium generated from wild-type astrocytes. Similar to wild-type neurons, MeCP2-null neurons showed aberrant dendritic morphology when cultured with conditioned medium from MeCP2-null astrocytes (Fig. 4e); when cultured with wild-type ACM, however, they appeared to be healthy and showed normal dendritic morphology (Fig. 4e). Furthermore, although 70% of the MeCP2-null neurons had short dendrites when cultured in mutant ACM, only 10% of the neurons had short dendrites when cultured with conditioned medium from wild-type astrocytes (Fig. 4f). Together, these results suggest that MeCP2 dysfunction in glia probably contributes to abnormal dendritic morphology of neurons in a non-cell autonomous fashion.

DISCUSSION

Increasing evidence supports the idea that glia of all types, including astrocytes, oligodendrocytes and microglia, each of which have close contact with neurons, help to support the neighboring neurons in various ways. For example, astrocytes, the major cellular component of the CNS, are important in synapse formation and plasticity and in preventing neuronal excitotoxicity by rapid removal of excess glutamate through glutamate transporters^{33,34}. Thus, it is perhaps not surprising that many neurodegenerative diseases, including amyotrophic lateral sclerosis, spinocerebellar ataxia, Huntington's disease, Parkinson's disease and multiple system atrophy, have recently been shown to have an astrocytic component. In these disorders, mutant products in astrocytes and microglia damage neighboring neurons, either by releasing toxic components or by mutant-mediated reduction in neuronal support functions²⁹. Astrocytes can also affect neurons indirectly. For example, multiple sclerosis, which is caused by oligodendrocyte degeneration, is initiated by and progresses in part because of astrocytes expressing toxic compounds, which then damage oligodendrocytes, leading to impaired neuronal signaling^{35,36}.

RTT is distinguished from these other neurodegenerative or neurological disorders in that it is initiated by a loss of MeCP2 function rather than by a gain of function of a toxic mutant protein. Although previous studies have focused on MeCP2 loss-of-function in the brain and specifically in neurons, its effects in the non-neuronal cells in the brain have generally been overlooked. Other *in vivo* experiments, however, suggested that further studies were warranted. Gene expression profiles of postmortem female RTT brains revealed decreased levels of expression of neuronal genes encoding synaptic markers and increased levels of expression of glial genes involved in neuropathological

mechanisms³⁷. Magnetic resonance imaging and spectroscopy studies showed that not only neuronal, but also glial, metabolism was affected in RTT mouse brain^{38,39}. Despite these changes, obvious neuronal and glial degeneration had not been reported in RTT⁴⁰ and the balance between neuronal and glial lineages produced from neural progenitors appeared normal²¹. Furthermore, the amounts of GFAP that are present in different regions of wild-type and RTT brains, as well as in astrocytic cultures from RTT and wild-type mice, are indistinguishable from each other (Supplementary Fig. 1 and data not shown), indicating that the number of astrocytes in RTT and wild-type brains is similar. These observations suggest that RTT is not caused by reduced cell numbers, but rather by dysfunction of specific cell types in the brain. Nonetheless, unlike mutant neurons, studies addressing the direct involvement of mutant glia in the neuropathology of RTT have been lacking, in part due to the uncertainty of the presence of MeCP2 in glia.

Our results indicate that MeCP2 is expressed not only in neurons, but in all types of glia of normal adult brain, whereas it is absent in glia of RTT brain. Notably, our coculture studies indicate that astrocytes from RTT male mice, as well as their conditioned medium, cause aberrant dendritic morphology in both mutant and wild-type neurons that resembles hippocampal pyramidal and granule cell abnormalities in conventional RTT male animals *in vivo*. This suggests that, in female human RTT patients, who are mosaic for loss of MeCP2 function, wild-type neurons are likely to be affected in a non-cell autonomous fashion by the mutant astrocytes. Supporting this notion is the finding that, in heterozygous human patients, the majority of pyramidal cortical neurons show aberrant dendritic morphology⁴¹. Furthermore, both RTT and wild-type neurons survive in culture and extend processes in the presence of conditioned medium from wild-type, but not mutant, astrocytes. This observation suggests that, consistent with *in vivo* studies, the damage to mutant neurons is not irreversible²⁰ and can potentially be rescued by therapeutic intervention.

Although aberrant dendritic morphology was the predominant effect of MeCP2-null astrocytes on the neurons, neuronal survival was, at least to some extent, also affected. Although it is generally accepted that RTT is not a neurodegenerative disorder, several earlier studies suggest that some neurodegeneration occurs in human RTT^{42,43}. Further studies are required to more systematically address whether mild neuronal degeneration occurs, at least in some circumstances, in RTT patients.

The astrocytic effect could be the result of a depletion of a molecule that is essential for neuronal dendritic morphology or of a soluble secreted factor that is detrimental to neurons. For example, depletion of neurotrophic factors such as glial cell line-derived neurotrophic factor, which affects dendritic branching, or molecules secreted from glia with deleterious effects such as tumor necrosis factor- α and nitric oxide, could cause aberrant morphology and/or loss in neuronal functions. By screening for several gene candidates whose aberrant expression could potentially perturb the levels of such essential molecules, we found that the expression of the branched-chain aminotransferase mRNA was upregulated threefold in MeCP2-null relative to wild-type astrocytic cultures. Branched-chain aminotransferase catalyzes the transamination of branched chain amino acids, the nitrogen donors for synthesis of glutamate in the brain, and can thus modulate the supply of glutamate. Further biochemical studies will determine whether a toxic factor is secreted from the mutant astrocytes. In this case, identification of the aberrantly secreted factor(s) could ultimately provide a means of pharmacological intervention for RTT.

Astrocytes in RTT animals could damage neurons through different non-cell autonomous pathways. It could either be that astrocytes are not directly affected by a loss of MeCP2 function, but rather the mutant

neurons stimulate damaging responses from glia that then affect the neurons, that astrocytes are affected directly by a loss of MeCP2 and this is the primary source of neurotoxicity, or that both astrocytes and neurons are affected directly by a loss of MeCP2, but a loss of MeCP2 from glia causes a glial damage response that enhances the initial damage in neurons. The latter scenario has precedence in amyotrophic lateral sclerosis; although mutant SOD1 expression in motor neurons is required for disease initiation, neurotoxicity is also produced by damage in the neighboring mutant glia, which facilitates the initiation and progression of the disease^{44,45}. Further *in vivo* studies are required to distinguish between these possible mechanisms. Toward this end, we are currently generating mouse models in which MeCP2-null astrocytes are produced in a background of wild-type neurons. Preliminary findings suggest that the selective loss of MeCP2 in astrocytes elicits, at least in part, an RTT-like phenotype.

METHODS

All animal studies were approved by the Institutional Animal Care and Use Committees at Stony Brook University and Oregon Health and Science University.

Primary cultures of rat glia. Rat glial cultures were prepared from cortices of P1–2 pups using the differential adhesion method^{46,47}. Cerebral cortices were digested in S-MEM (Gibco) containing 0.1% trypsin (vol/wt, Worthington) and triturated with 60 $\mu\text{g ml}^{-1}$ DNase I (Sigma) and 10% fetal bovine serum (FBS, vol/vol, Gibco). Dissociated cells from 2–3 pups were plated in a 75-cm² tissue culture flask coated with 100 $\mu\text{g ml}^{-1}$ poly-L-lysine (Sigma) in DMEM containing 10% FBS and 2 mM glutamine. After 10 d, with a medium change every 3 d, the flasks were sealed and shaken at 250 rpm at 37 °C for 15–18 h followed by an additional 30 min at 350 rpm. Adherent cells (astrocytes) were dissociated with 0.1% trypsin and passaged using the same medium. Detached cells were collected and plated on tissue culture dishes for 30 min at 37 °C to eliminate contaminating astrocytes and microglia. The nonadherent cells (OPCs) were collected and replated overnight in DMEM containing 10% FBS at densities of 6,000–8,000 cells per cm² in tissue culture dishes or coverslips coated with 10 $\mu\text{g ml}^{-1}$ poly-L-lysine, after which the medium was replaced with B27/NB-A (Gibco) medium containing 10 ng ml⁻¹ platelet-derived growth factor and fibroblast growth factor. For oligodendrocyte differentiation, growth factors were withdrawn from the medium after 3 d and replaced with DMEM containing 0.5% FBS, N1 (Gibco), 30 ng ml⁻¹ T3 and 40 ng ml⁻¹ T4 (Sigma). Under these conditions, enriched glial cultures contained >95% GFAP-positive astrocytes, ~90% NG2-positive OPCs and ~85% MBP-positive oligodendrocytes.

Culturing mouse astrocytes and preparation of ACM. Cortices from P1–2 MeCP2 mutant and wild-type male littermates were dissociated in S-MEM medium (Gibco) containing 20 U ml⁻¹ papain (Worthington), 0.25 mg ml⁻¹ L-cysteine and 40 $\mu\text{g ml}^{-1}$ DNase (Sigma). Papain was inactivated with L15 medium containing 50 $\mu\text{g ml}^{-1}$ BSA, 40 $\mu\text{g ml}^{-1}$ DNase and 1 mg ml⁻¹ soybean trypsin inhibitor (Sigma). Cortices were triturated and plated on 100 $\mu\text{g ml}^{-1}$ poly-L-lysine-coated 25-cm² tissue culture flasks in DMEM medium containing 10% FBS and 2 mM glutamine. When confluent (after 6–7 d), astrocytes were dissociated with TrypLE (Gibco) and passaged to a 10-cm poly-L-lysine-coated flask. To generate ACM, we plated astrocytes in the second passage onto poly-L-lysine-coated 10-cm tissue culture dishes. When cultures were >95% confluent, the medium was completely replaced with serum-free neuronal maintenance medium³² as described. Over 95% of the cells were GFAP positive in both MeCP2 mutant and MeCP2 wild-type cultures. ‘Conditioned’ neuronal maintenance media were collected at 7 and 14 d, combined, centrifuged at 1000g for 5 min, filtered, sorted into aliquots and stored at –80 °C.

Hippocampal neuron and astrocyte cocultures. Unless otherwise stated, all of the coculture experiments were performed with astrocytes and neurons isolated from the same MeCP2 mouse model¹⁵. Hippocampi from P1 MeCP2 mutant and wild-type male littermates were dissociated with papain as described above for mouse astrocytes. The coculture of the neurons with astrocytes was

performed as described previously³². Hippocampal neurons (80,000 standard density) in neuronal plating medium were plated onto each coverslip containing paraffin dots and coated with 0.5 mg ml⁻¹ poly-L-lysine³². When neurons adhered (after 3–4 h), medium was discarded and coverslips were inverted and placed in a 12-well dish containing a monolayer of astrocytes (50–60% confluence) in a serum-free neuronal maintenance medium³². Cytosine arabinoside (2 μM) was added 3 d after plating to limit glial proliferation. For culturing hippocampal neurons in ACM, neurons were plated on coverslips as described above at standard density or low density (40,000), but without paraffin dots. After neurons adhered, neuronal plating medium was replaced with 1 ml of a 1:1 mixture of ACM and neuronal maintenance medium. Cytosine arabinoside was added as described above.

Transfection of hippocampal neurons with GFP expression vector. Hippocampal neurons cultured in ACM (3 d *in vitro*, DIV) were transfected with the pmaxCloning vector (Amara) containing GFP coding sequences under the control of the CMV promoter. We incubated 4 μl of lipofectamine 2000 (Invitrogen) in 100 μl MEM (GIBCO) for 5 min at 22–25 °C and added to an equal volume of MEM containing 0.1 μg of DNA. Following a 30-min incubation at 22–25 °C, the DNA/lipofectamine mix was added to the neurons, after the removal of the ACM, for 90 min at 37 °C, after which it was replaced with fresh ACM. After 24 h, GFP was visible in approximately 0.1% of the neurons.

RNA isolation and quantitative real-time PCR analysis. Total RNA was prepared from cells using RNeasy (Qiagen) and treated with RNase-free DNase (Ambion, DNA-free kit). For reverse transcription, First Strand Superscript II (Invitrogen) was used and quantitative real-time PCR was performed in an ABI PRISM 7700 Sequence Detector using SYBR-green PCR master mix (PE Applied Biosystem). The relative abundance of the specific mRNAs was normalized to *Gapdh* mRNA. For quantitative real-time RT-PCR, we used two *Mecp2* primers, forward 5'-AAG AGG GCA AAC ATG AAC CAC T-3' and reverse 5'-TTG CCT GCC TCT GCT GG-3', and two *GAPDH* primers, forward 5'-AAG TAT GAT GAC ATC AAG AAG GTG GT-3' and reverse 5'-AGC CCA GGA TGC CCT TTA GT-3'.

Immunocytochemistry. Cells were fixed with 4% paraformaldehyde (wt/vol) and probed with rabbit antibody to MeCP2 (a generous gift from M. Greenberg, Harvard Medical School), mouse antibody to MAP2 (Chemicon), mouse antibody to MBP (Chemicon), mouse antibody to GFAP (Chemicon) or mouse antibody to neuronal β -tubulin (TUJ1, Chemicon), followed by incubation with the appropriate secondary antibody conjugated to Alexa Fluor (Molecular Probes)⁴⁸. For NG2 staining, mouse antibody to NG2 (a generous gift from J. Levine, Stony Brook University) in L15 medium was applied to living cells for 45 min, after which the cells were washed and fixed as above. In this case, a second primary antibody was applied sequentially after fixation and cells were probed with the secondary antibodies described above. Images were collected on a Zeiss confocal laser scanning LSM 510 microscope.

Immunohistochemistry. Mice or rats were killed by transcardial perfusion with 4% paraformaldehyde in phosphate-buffered saline. Brains were cryoprotected overnight in 30% sucrose and coronal sections were cut (40 μm) on a freezing microtome (Bright Instruments). Sections were immunostained using antibodies to MeCP2 and GFAP as described above, mouse antibody to RIP (Chemicon), guinea pig antibody to NG2 (a generous gift from W. Stallcup, Burnham Institute), or mouse antibody to NeuN (Chemicon), followed by incubation with secondary antibodies conjugated to cyanine (Jackson ImmunoResearch). MeCP2 immunostaining was enhanced using biotin-streptavidin-conjugated secondary antibodies. Images were collected on a Zeiss confocal laser scanning LSM 510 microscope.

Whole cell protein extraction, histone extraction and western blot analysis. Nuclear and cytoplasmic cell extracts were prepared using the modified Dignam method⁴⁹. For whole cell extracts, cells were lysed directly in nuclear lysis buffer. Histone extraction was performed using the acid extraction method⁵⁰. For western blot analysis, we used antibody to MeCP2 and antibody to Sin3A, as described above, mouse antibody to Neurofilament-L (Cell Signaling), mouse antibody to α -tubulin (Sigma), rabbit antibodies to

trimethyl-histone H3 lysine 9 and acetyl histone H3 (Upstate), and rabbit antibody to histone H3 (Abcam).

Note: Supplementary information is available on the Nature Neuroscience website.

ACKNOWLEDGMENTS

The authors thank J. Levine and L. Evans for providing the enriched glial cultures for the initial immunostaining analysis; P. Brehm, R. Goodman, T. Reese and G. Banker for valuable discussions about the results; and D.D. Lu and R. Spektor for technical assistance. This work was supported in part by a grant from the International Rett Syndrome Foundation to N.B. and a US National Institutes of Health grant to G.M. and N.B. G.M. is an Investigator of the Howard Hughes Medical Institute.

AUTHOR CONTRIBUTIONS

N.B., D.T.L., C.G. and G.M. designed the experiments. N.B., D.T.L. and C.G. carried out the experiments. N.B., D.T.L. and G.M. wrote the paper. N.B. and G.M. supervised the project.

Published online at <http://www.nature.com/natureneuroscience/>

Reprints and permissions information is available online at <http://npg.nature.com/reprintsandpermissions/>

- Amir, R.E. *et al.* Rett syndrome is caused by mutations in X-linked MECP2, encoding methyl-CpG-binding protein 2. *Nat. Genet.* **23**, 185–188 (1999).
- Chahrour, M. & Zoghbi, H.Y. The story of Rett syndrome: from clinic to neurobiology. *Neuron* **56**, 422–437 (2007).
- Chandler, S.P., Guschin, D., Landsberger, N. & Wolffe, A.P. The methyl-CpG binding transcriptional repressor MeCP2 stably associates with nucleosomal DNA. *Biochemistry* **38**, 7008–7018 (1999).
- Kriaucionis, S. & Bird, A. DNA methylation and Rett syndrome. *Hum. Mol. Genet.* **12**, R221–R227 (2003).
- Harikrishnan, K.N. *et al.* Brahma links the SWI/SNF chromatin-remodeling complex with MeCP2-dependent transcriptional silencing. *Nat. Genet.* **37**, 254–264 (2005).
- Jones, P.L. *et al.* Methylated DNA and MeCP2 recruit histone deacetylase to repress transcription. *Nat. Genet.* **19**, 187–191 (1998).
- Nan, X. *et al.* Transcriptional repression by the methyl-CpG-binding protein MeCP2 involves a histone deacetylase complex. *Nature* **393**, 386–389 (1998).
- Fuks, F. *et al.* The methyl-CpG-binding protein MeCP2 links DNA methylation to histone methylation. *J. Biol. Chem.* **278**, 4035–4040 (2003).
- Chen, W.G. *et al.* Derepression of BDNF transcription involves calcium-dependent phosphorylation of MeCP2. *Science* **302**, 885–889 (2003).
- Martinowich, K. *et al.* DNA methylation-related chromatin remodeling in activity-dependent BDNF gene regulation. *Science* **302**, 890–893 (2003).
- Zhou, Z. *et al.* Brain-specific phosphorylation of MeCP2 regulates activity-dependent Bdnf transcription, dendritic growth and spine maturation. *Neuron* **52**, 255–269 (2006).
- Yasui, D.H. *et al.* Integrated epigenomic analyses of neuronal MeCP2 reveal a role for long-range interaction with active genes. *Proc. Natl. Acad. Sci. USA* **104**, 19416–19421 (2007).
- Chahrour, M. *et al.* MeCP2, a key contributor to neurological disease, activates and represses transcription. *Science* **320**, 1224–1229 (2008).
- Young, J.I. *et al.* Regulation of RNA splicing by the methylation-dependent transcriptional repressor methyl-CpG-binding protein 2. *Proc. Natl. Acad. Sci. USA* **102**, 17551–17558 (2005).
- Chen, R.Z., Akbarian, S., Tudor, M. & Jaenisch, R. Deficiency of methyl-CpG-binding protein 2 in CNS neurons results in a Rett-like phenotype in mice. *Nat. Genet.* **27**, 327–331 (2001).
- Guy, J., Hendrich, B., Holmes, M., Martin, J.E. & Bird, A. A mouse Mecp2-null mutation causes neurological symptoms that mimic Rett syndrome. *Nat. Genet.* **27**, 322–326 (2001).
- Shahbazian, M. *et al.* Mice with truncated MeCP2 recapitulate many Rett syndrome features and display hyperacetylation of histone H3. *Neuron* **35**, 243–254 (2002).
- Gemelli, T. *et al.* Postnatal loss of methyl-CpG binding protein 2 in the forebrain is sufficient to mediate behavioral aspects of Rett syndrome in mice. *Biol. Psychiatry* **59**, 468–476 (2006).
- Giacometti, E., Luikenhuis, S., Beard, C. & Jaenisch, R. Partial rescue of MeCP2 deficiency by postnatal activation of MeCP2. *Proc. Natl. Acad. Sci. USA* **104**, 1931–1936 (2007).
- Guy, J., Gan, J., Selfridge, J., Cobb, S. & Bird, A. Reversal of neurological defects in a mouse model of Rett syndrome. *Science* **315**, 1143–1147 (2007).
- Kishi, N. & Macklis, J.D. MECP2 is progressively expressed in post-migratory neurons and is involved in neuronal maturation rather than cell fate decisions. *Mol. Cell. Neurosci.* **27**, 306–321 (2004).
- Armstrong, D.D. Neuropathology of Rett syndrome. *J. Child Neurol.* **20**, 747–753 (2005).
- Belichenko, P.V., Oldfors, A., Hagberg, B. & Dahlstrom, A. Rett syndrome: 3-D confocal microscopy of cortical pyramidal dendrites and afferents. *Neuroreport* **5**, 1509–1513 (1994).
- Moretti, P. *et al.* Learning and memory and synaptic plasticity are impaired in a mouse model of Rett syndrome. *J. Neurosci.* **26**, 319–327 (2006).
- Asaka, Y., Jugloff, D.G., Zhang, L., Eubanks, J.H. & Fitzsimonds, R.M. Hippocampal synaptic plasticity is impaired in the Mecp2-null mouse model of Rett syndrome. *Neurobiol. Dis.* **21**, 217–227 (2006).
- Chao, H.T., Zoghbi, H.Y. & Rosenmund, C. MeCP2 controls excitatory synaptic strength by regulating glutamatergic synapse number. *Neuron* **56**, 58–65 (2007).
- Dani, V.S. *et al.* Reduced cortical activity due to a shift in the balance between excitation and inhibition in a mouse model of Rett syndrome. *Proc. Natl. Acad. Sci. USA* **102**, 12560–12565 (2005).
- Jung, B.P. *et al.* The expression of methyl CpG binding factor MeCP2 correlates with cellular differentiation in the developing rat brain and in cultured cells. *J. Neurobiol.* **55**, 86–96 (2003).
- Lobsiger, C.S. & Cleveland, D.W. Glial cells as intrinsic components of non-cell autonomous neurodegenerative disease. *Nat. Neurosci.* **10**, 1355–1360 (2007).
- Thatcher, K.N. & LaSalle, J.M. Dynamic changes in histone H3 lysine 9 acetylation localization patterns during neuronal maturation require MeCP2. *Epigenetics* **1**, 24–31 (2006).
- Banker, G.A. Trophic interactions between astroglial cells and hippocampal neurons in culture. *Science* **209**, 809–810 (1980).
- Kaech, S. & Banker, G. Culturing hippocampal neurons. *Nat. Protoc.* **1**, 2406–2415 (2006).
- Ullian, E.M., Sapperstein, S.K., Christopherson, K.S. & Barres, B.A. Control of synapse number by glia. *Science* **291**, 657–661 (2001).
- Maragakis, N.J. & Rothstein, J.D. Glutamate transporters in neurologic disease. *Arch. Neurol.* **58**, 365–370 (2001).
- Antony, J.M. *et al.* Human endogenous retrovirus glycoprotein-mediated induction of redox reactants causes oligodendrocyte death and demyelination. *Nat. Neurosci.* **7**, 1088–1095 (2004).
- Back, S.A. *et al.* Hyaluronan accumulates in demyelinated lesions and inhibits oligodendrocyte progenitor maturation. *Nat. Med.* **11**, 966–972 (2005).
- Colantuoni, C. *et al.* Gene expression profiling in postmortem Rett syndrome brain: differential gene expression and patient classification. *Neurobiol. Dis.* **8**, 847–865 (2001).
- Saywell, V. *et al.* Brain magnetic resonance study of Mecp2 deletion effects on anatomy and metabolism. *Biochem. Biophys. Res. Commun.* **340**, 776–783 (2006).
- Viola, A., Saywell, V., Villard, L., Cozzone, P.J. & Lutz, N.W. Metabolic fingerprints of altered brain growth, osmoregulation and neurotransmission in a Rett syndrome model. *PLoS ONE* **2**, e157 (2007).
- Jellinger, K., Armstrong, D., Zoghbi, H.Y. & Percy, A.K. Neuropathology of Rett syndrome. *Acta Neuropathol.* **76**, 142–158 (1988).
- Armstrong, D., Dunn, J.K., Antalffy, B. & Trivedi, R. Selective dendritic alterations in the cortex of Rett syndrome. *J. Neuropathol. Exp. Neurol.* **54**, 195–201 (1995).
- Hanefeld, F. *et al.* Cerebral proton magnetic resonance spectroscopy in Rett syndrome. *Neuropediatrics* **26**, 126–127 (1995).
- Kitt, C.A. & Wilcox, B.J. Preliminary evidence for neurodegenerative changes in the substantia nigra of Rett syndrome. *Neuropediatrics* **26**, 114–118 (1995).
- Clement, A.M. *et al.* Wild-type nonneuronal cells extend survival of SOD1 mutant motor neurons in ALS mice. *Science* **302**, 113–117 (2003).
- Yamanaka, K. *et al.* Mutant SOD1 in cell types other than motor neurons and oligodendrocytes accelerates onset of disease in ALS mice. *Proc. Natl. Acad. Sci. USA* **105**, 7594–7599 (2008).
- McCarthy, K.D. & de Vellis, J. Preparation of separate astroglial and oligodendroglial cell cultures from rat cerebral tissue. *J. Cell Biol.* **85**, 890–902 (1980).
- Yang, Z., Watanabe, M. & Nishiyama, A. Optimization of oligodendrocyte progenitor cell culture method for enhanced survival. *J. Neurosci. Methods* **149**, 50–56 (2005).
- Ballas, N. *et al.* Regulation of neuronal traits by a novel transcriptional complex. *Neuron* **31**, 353–365 (2001).
- Grimes, J.A. *et al.* The co-repressor mSin3A is a functional component of the REST-CoREST repressor complex. *J. Biol. Chem.* **275**, 9461–9467 (2000).
- Shechter, D., Dormann, H.L., Allis, C.D. & Hake, S.B. Extraction, purification and analysis of histones. *Nat. Protoc.* **2**, 1445–1457 (2007).